

Influence of Phenolic Compounds on Antioxidant and Anticorrosion Activities of *Ammi visnaga* Extracts Obtained Ultrasonically in Three Solvent Systems

S. Aourabi^{1,2,*}, M. Driouch², M. Sfaira², F. Mahjoubi¹, B. Hammouti³, K.M. Emran^{4,*}

¹Laboratoire de Génie des Matériaux et Environnement, Faculté des Sciences, Université Sidi Mohamed Ben Abdellah (USMBA), B.P. 1796-30000, Fès-Atlas, Morocco.

²Laboratoire d'Ingénierie des Matériaux, de Modélisation et d'Environnement. Université Sidi Mohamed Ben Abdellah (USMBA), Faculté des Sciences B.P. 1796-30000, Fès-Atlas, Morocco.

³Laboratoire de la chimie appliquée et d'environnement, Faculté des sciences, Université Mohammed Premier, BP 4808 Oujda, Morocco.

⁴ Department of Chemistry, College of Science, Taibah University, Al-Madinah Al-Monawarah, PO Box 4050, Saudi Arabia

*E-mail: kabdalsamad@taibahu.edu.sa & sarra.aourabi@gmail.com

Received: 15 February 2019/ Accepted: 23 April 2019 / Published: 10 June 2019

The purpose of this research was to study the correlation between phenolic compounds and antioxidant as well as anticorrosive activities of different extracts of *Ammi visnaga*. The antioxidant capacity was evaluated by 2,2-diphenyl-1-picrylhydrazyl (DPPH[•]). The phenolic compounds, namely, total phenol content (TPC), total flavonoids content (TFC), and condensed tannins (CT), were determined by Folin–Ciocalteu, Quettier–Deleu, and Broadhurst methods, respectively. In addition, the inhibiting effect of different extracts of *A. visnaga* on mild steel in 1 M HCl solution was investigated by potentiodynamic polarization (PP) and electrochemical impedance spectroscopy (EIS). The obtained results revealed that the mixed aqueous extract had a high level of phenolic compounds when compared with pure solvents. Hydroalcoholic extract had the highest radical trapping capacity ($IC_{50} = 1.7$ mg/mL) compared with standard butylated hydroxytoluene (BHT) ($IC_{50} = 0.2$ mg/mL). The PP tests showed that the extracts act as mixed inhibitors, whereas EIS measurements indicated that action inhibition of mild steel can be explained by the adsorption of active compounds at the metal surface. The trends between condensed tannins and antioxidant activity, as well as the inhibition efficiency derived from Tafel plots and EIS, were revealed, respectively.

Keywords: *Ammi visnaga* extract; TPC; TFC; condensed tannins; antioxidant activity; corrosion inhibition.

1. INTRODUCTION

Ammi visnaga is a perennial plant belonging to the umbelliferae (Apiaceae) family. It is widely distributed in North Africa, Europe, the Eastern Mediterranean region, southwestern, Asia, North America, Argentina, Chile, Mexico, and Atlantic islands [1]. The main active constituents of this genus are coumarin and its derivatives, flavonoids, and furanochromone [2]. All flavonoids described in *Ammi* species can be classified into flavonols (quercetin, kaempferol, and isorhamnetin) and flavones (apigenin, luteolin, and chrysoeriol). These types of flavonoids have been shown to be powerful antioxidants and free radical scavengers [3-5].

The contents of these compounds in dried fruits varies widely according to genetic factors and environmental conditions [6]. The yield of phenolic compounds in the extract depends on several factors: type of solvent, extraction method, extraction time, temperature, composition, as well as physical characteristics of the sample, such as texture [7]. Several different methods are available and have been used to assess the antioxidant activity of plant extracts, including the 2,2'-azinobis (3-ethylbenzothiazoline-6-sulphonic acid) diammonium salt (ABTS) assay [8], the total antioxidant capacity (TAC), the 1,1-diphenyl-2-picrylhydrazyl (DPPH[•]) test [9], and the ferric-reducing antioxidant power (FRAP) assay [10]. Previous studies [9, 8, 11] have used only one assay method to assess the total antioxidant activity of plant extracts. In the present study, we evaluated the antioxidant activity of different extracts by DPPH[•] assays. The DPPH[•] method is preferred because it is fast, stable, easy, reliable, and does not require a special reaction and device.

On the other hand, several studies have investigated mild steel corrosion in acidic environments because of its many applications in the industrial field. However, its susceptibility to rusting in humid air as well as its high dissolution rate in acidic solutions are the major obstacles for its use on a larger scale without protection. Electrochemical corrosion is generally caused by the potentials between the metal and a strong acid. The aggressiveness of hydrogen ions and dissolved oxygen are referred to as natural motors of corrosion [12,13]. Due to this problem, corrosion inhibitors are required. Indeed, many synthetic compounds have been studied as corrosion inhibitors [14-16], which offer good anticorrosive action, but most of them risk being highly toxic to both humans and the environment. In the last decade, researchers have evaluated the use of ecofriendly compounds, as green corrosion inhibitors, of mild steels to replace toxic chemicals currently in use. Indeed, several studies have been carried out on corrosion inhibition by using essential oils [17,18] and plant extracts [19-23]. All of them have been reported to be good inhibitors for various metals and alloys in different acidic media.

The focus of this work is to study the correlation between phenolic compounds of different extracts of *A. visnaga* and their antioxidant and corrosion inhibition properties. Furthermore, the impact of solvents, namely, water, ethanol, and ethanol/water, is also taken into account. Corrosion behavior is evaluated by potentiodynamic polarization (PP) and electrochemical impedance spectroscopy (EIS).

2. EXPERIMENTAL PART

2.1. *A. visnaga* was collected from the Taounate region of Morocco in July 2017. The botanical identification of the species was carried out in the Laboratory of Biotechnology and Preservation of Natural Resources (BPNR), Sidi Mohamed Ben Abdellah University, Fez, Morocco. The extracts were obtained ultrasonically, mixing the dry powder with different solvents (water, ethanol, and ethanol/water) for 45 min at 308 K. The extracts were filtered and concentrated under reduced pressure.

2.1.1. Screening phytochemical analysis

The qualitative phytochemistry of the dry extract was achieved by colorimetric reactions and precipitation by specific chemical reagents according to the protocols given in the literature [24-26]. These tests revealed the presence of a number of compound groups of the three extracts.

2.1.2. Determination of Total Phenol Content (TPC)

The TPC of the extracts was investigated by the Folin–Ciocalteu method [27]. This method provided the total polyphenolic content of a given sample. The plant extract (100 μ L), suitably diluted, was introduced into a test tube initially containing 6 mL of distilled water, then 500 μ L of the Folin reagent was added and the mixture was stirred. After 5 min, a solution of 20% Na_2CO_3 (1.5 mL) was added while stirring.

The solution was adapted to 10 mL with distilled water. The absorbance of the sample was measured at 760 nm against water using a spectrophotometer UV–Visible kind Selecta after 2 h of incubation at room temperature. A calibration curve at different concentrations of gallic acid was plotted. The total phenol content in the extract was expressed by mg EGA/g of extract.

2.1.3. Determination of Total Flavonoids Content (TFC)

The total flavonoids content of various extracts of *A. visnaga* was determined by the Quettier–Deleu method [28]. The method consists of mixing 1 mL of the extract with an equal volume of a solution of $\text{AlCl}_3 \cdot 6\text{H}_2\text{O}$ (2%). After 10 min, the absorbance of the mixture was measured at 430 nm. The quantification of flavonoids was determined based on a linear calibration curve performed by quercetin at different concentrations. The results were expressed in milligrams equivalent to quercetin per gram of extract (mg EQ/g of extract).

2.1.4. Determination of Condensed Tannins (CT)

Condensed tannins (proanthocyanidins) were determined according to the Sun method [29], with a slight modification. Four hundred microliters of extract were added to 1.5 mL of concentrated hydrochloric acid and 3 mL of a solution of vanillin (4% in methanol). After 15 min of incubation at room temperature, the absorbance was measured at 500 nm against methanol as a blank. The amount of total condensed tannins was expressed in milligrams equivalent to catechin per gram of extract.

counter electrode. The working electrode was immersed in 50 mL of the test solution during 30 min in open circuit potential (E_{ocp}) to obtain a stable potential.

The potentiodynamic polarization for mild steel in the test solution in the absence or presence of various extract inhibitions were recorded from -900 to -100 mV with a scanning rate of 1 mV s^{-1} . The corrosion parameters, such as cathodic Tafel slope (β_c), corrosion current density (i_{corr}), and corrosion potential (E_{corr}), were evaluated by using Ec-Lab software.

Impedance spectra were recorded in the frequency range from 100 kHz to 100 mHz with 10 points per decade at 308 K at an alternating current amplitude of ± 10 mV ac voltage peak to peak. The impedance spectra, given in the Nyquist and Bode representations, were analyzed in terms of an appropriate equivalent electrical circuit implemented in Ec-Lab software. All experiments were repeated three times.

3. RESULTS AND DISCUSSION

3.1. Extraction yield of various extracts of *A. visnaga*

The results of the ultrasonic extraction efficiency by three solvents are given in Table 1. The results of the ultrasonic extraction yield of different extracts of *A. visnaga* showed that the hydroalcoholic extract gave the highest value of 16.24%, followed by the aqueous extract, which gave a yield of 12.35%. Thus, the use of mixed solvents led to high enrichment of extracts with polyphenols [31]. The superiority of these solvents could be due to the increased solubility of phenolic compounds in mixed solvents when compared with pure solvents [32, 33].

Table 1. Solvent effects on the extraction yield of *Ammi visnaga*.

Solvent	Solvent polarity*	Extraction yield (%)
Water	10.2	12.35
Ethanol	5.2	9.12
Hydroalcoholic (70:30 v/v Ethanol-Water)	6.7	16.24

* The solvent mixture indexes were calculated from the equation $\left(\frac{I_w}{100} \times P_w\right) + \left(\frac{I_E}{100} \times P_E\right)$, where I_w and I_E are the polarity indexes of the solvents water and ethanol, respectively, and P_w and P_E are the percentage of solvents water and ethanol, respectively, in the solvent mixture [7].

The results showed those phenolic molecules were more soluble in polar solvents than in nonpolar solvents. A considerable rise in extract yield was observed by the combination of water and an organic solvent system. The yield was more important with a solvent mixture compared with the solvents taken separately. Indeed, phenolic compounds are highly soluble in a mixture of organic and polar (water) solvents. Similar results were obtained by Ammor and Aourabi [34, 35], and the extraction yield of the hydroalcoholic and ethanolic extract of *A. visnaga* obtained by Soxhlet gave values of 23.40% and 23.35%, respectively. The extracts obtained by ultrasonic extraction had low yields compared with those obtained by Soxhlet; this can be explained by the heating applied during the operation (Soxhlet)

as well as the long extraction time. Hence, the extraction method as well as the type of solvent significantly influenced the extraction efficiency.

3.2. Screening phytochemical analysis

According to Table 2, the screening phytochemical carried out on the various extracts of *A. visnaga* showed the presence of condensed tannins, flavonoids, and coumarins in all extracts. Alkaloids appeared only in aqueous and hydroalcoholic extracts. However, anthocyanins, leucoanthocyanins, cardiac glycosides, monosaccharides, and holosides were absent in all three extracts.

Table 2. Screening phytochemical of three extracts of *A. visnaga*.

Chemical constituent		Hydroalcoholic	Aqueous	Ethanollic	
Polyphenols	Tannins	Total tannins	+	+	+
		Gallic tannins	-	-	-
		Catechin tannins	+	+	+
	Flavonoids	Flavonols	+	+	+
		Anthocyanes	-	-	-
		Leucoanthocyanes	-	-	-
Alcaloids		+	-	+	
Mucilage		-	-	-	
Saponosids		-	-	-	
Coumarins		+	+	+	
Cardiac glycosides		-	-	-	
Monosaccharides and holosides		-	-	-	

+: presence and -: absence

3.3. Determination of TPC

The phenolic content in different samples was influenced by the polarity of the solvent as well as the solubility of these compounds in the solvent used for extraction [34, 36]. The TPC values were obtained from the calibration curve equation (2):

$$Y = 0.564x + 0.176 \quad R^2 = 0.997 \quad (2)$$

where Y is the absorbance and x is the concentration of the gallic acid solution (mg/mL).

The TPC values in different extracts of *A. visnaga* are shown in Table 3. The TPC values of the extracts varied from 69 to 110 mg EGA/g extract. The TPC extracted by the various solvents can be

classified in descending order: hydroalcoholic > ethanolic > aqueous. These results indicate that 70% of ethanol produced a greater phenolic yield than the other selected solvents. It should be noted that there was a trend between TPC and extraction efficiency, with the exception of the solvent ethanol, which gave a relatively high TPC value compared to its extraction capacity.

3.4. Determination of TFC

The content of flavonoids was determined by colorimetric reactions and the results are reported in Table 3. The TFC of the extracts ranged from 18 to 34 mg of EQ/g extract in descending order: hydroalcoholic > ethanolic > aqueous. The TFC values were lower than the TPC values, which is logical because flavonoids are subclasses of polyphenolic compounds.

The obtained results were superior to [34] because the content of phenolic compounds varied by the extraction method according to [37]. The extraction of phenolic compounds by the combination of alcohol and water was more efficient when compared with extraction by a single solvent [38], and the present results were in agreement with those found by [39, 40].

3.5. Determination of CT

Tannins can be classified into two groups, namely, hydrolysable and condensed tannins [41]. As seen in Table 3, the extracts had a high CT content, ranging from 20 to 65 mg of catechin/g extract. The results showed that the hydroalcoholic extract was characterized by a higher content of CT followed by ethanolic and aqueous extracts.

Table 3. Contents of TPC, TFC, and CT in different extracts of *A. visnaga*.

Extract	TPC (mg EGA/g extract)	TFC (mg EQ/g extract)	CT (mg catechin/g extract)
Aqueous	69.33±0.08	18.60±0.04	20.00±0.09
Ethanolic	77.09±0.02	22.51±0.01	44.30±0.02
Hydroalcoholic	110.02±0.02	34.50±0.09	65.20±0.24

* Data are expressed as means ± standard deviation of triplicate samples

3.6. Determination of antioxidant activity by the DPPH[•] method

The antioxidant activities of extracts depend on the ability of antioxidant compounds to lose hydrogen [42,43]. The DPPH[•] free radical, which is at its maximum wavelength of 517 nm, can easily receive an electron or hydrogen from antioxidant molecules to become a stable diamagnetic molecule [44].

The free radical scavenging effects of different concentrations of aqueous, ethanolic, and hydroalcoholic extracts of *Ammi visnaga* along with BHT and ascorbic acid are reported in Figure 2. The antioxidant activity of the extracts was compared to BHT and ascorbic acid as synthetic antioxidants.

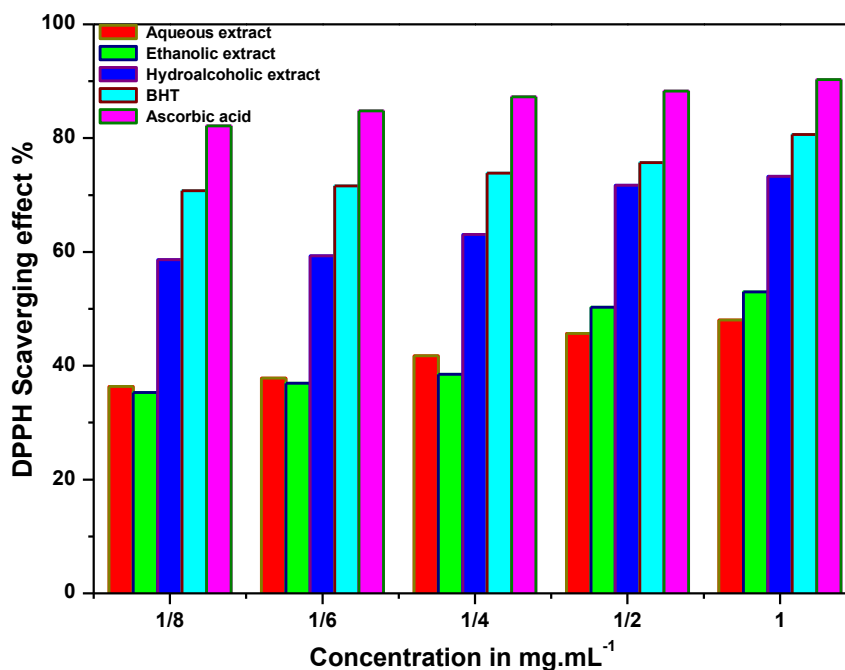


Figure 2. Antioxidant capacity of different extracts of *A. visnaga* and reference standard by the DPPH[•] method.

The free radical scavenging effects of different concentrations of aqueous, ethanolic, and hydroalcoholic extracts of *A. visnaga* along with BHT and ascorbic acid are reported in Figure 2. The antioxidant activity of the extracts was compared to BHT and ascorbic acid as synthetic antioxidants.

It can be seen from Fig. 2 that for concentrations of 1, 1/2, and 1/4 mg/mL, the percentage of DPPH[•] scavenging effects of the aqueous extract decreased, under the present experimental conditions, till 48.6%, 45.1%, and 41.7%, respectively. The ethanolic extract decreased until 52.23%, 50.42%, and 38.34%, respectively, and for the hydroalcoholic extract, the decrease was as high as 73.28%, 71.70%, and 63.04% when compared with BHT with the corresponding values of 80.62%, 75.72%, and 73.83%, as well as for the ascorbic acid with 90.30%, 88.27%, and 87.23%. A similar tendency was registered for 1/6 and 1/8 mg/mL.

As shown in Table 4, the IC_{50} found in this study for the hydroalcoholic extract of *A. visnaga* was as high as 1.7 mg/mL, followed by the ethanolic extract with 2.4 mg/mL, whereas 3.05 is obtained for the aqueous extract when compared to 0.24 and 0.19 mg/mL for BHT and ascorbic acid, respectively. The high capacity of the hydroalcoholic extract to trap free radicals could be attributed to the presence of a high polyphenol content according to [45, 46]. Our results were in agreement with other researchers [34, 40].

From these results, it can therefore be concluded that the antioxidant activity of the extract was closely dependent on the selected solvent [47].

Table 4. Comparison of antioxidant properties of different extracts of *Ammi visnaga* and reference standard.

Extract	IC_{50} (mg mL ⁻¹)
Aqueous	3.05
Ethanollic	2.40
Hydroalcoholic	1.70
BHT	0.24
Ascorbic acid	0.19

3.7. Correlation between antioxidant activity and phenolic compounds

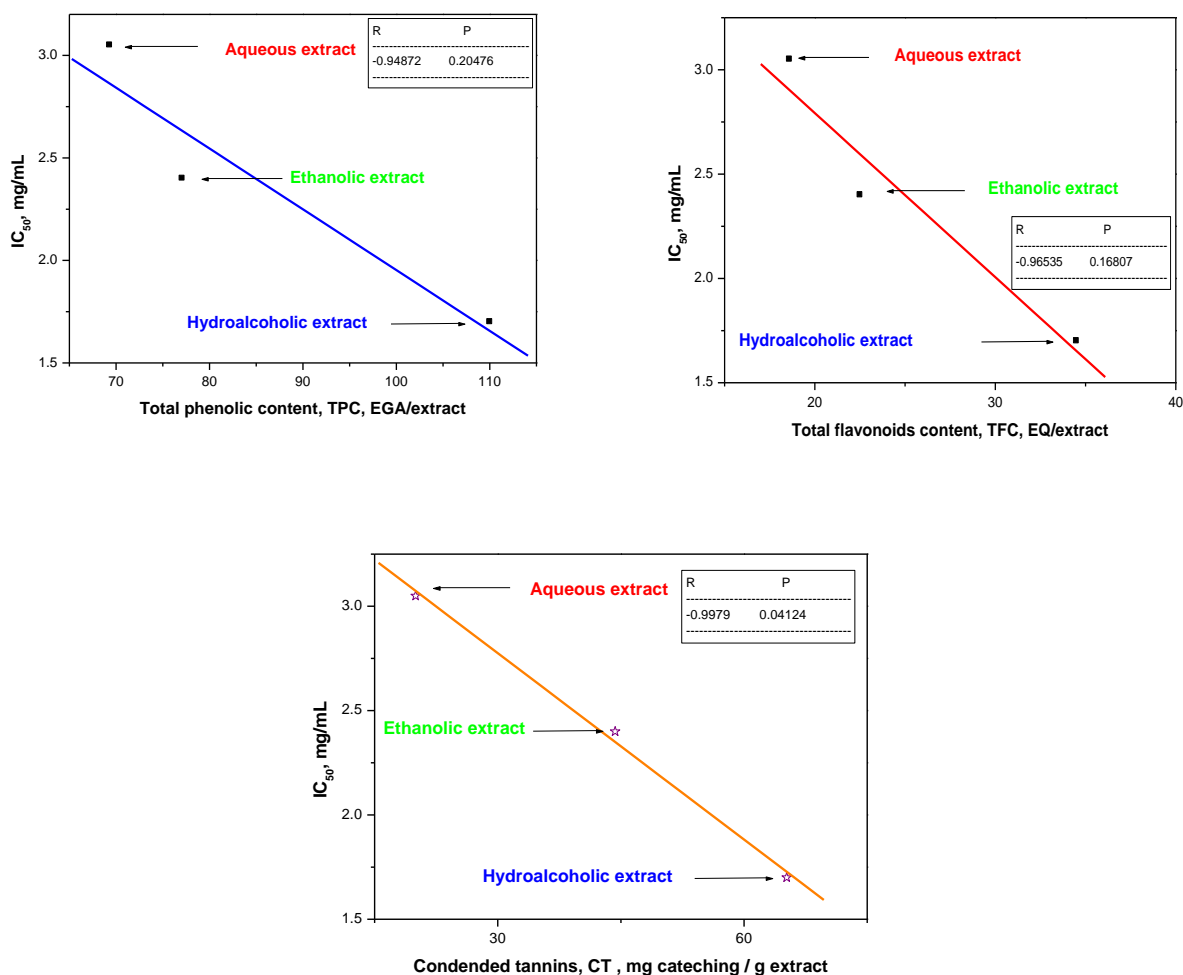


Figure 3. Correlation between IC_{50} and TFC, CT and TPC of different extracts of *Ammi visnaga*

Figure 3 exemplifies the relationship between antioxidant activity IC_{50} and TPC, TFC, and CT measured in various extracts of *Ammi visnaga*. It can obviously be seen that there was a linear correlation between the antioxidant activity determined by the DPPH[•] method and phenolic compounds with the

following determination coefficients: $R^2 = 0.9001$, 0.9319 , and 0.9958 , respectively. Besides, a strong correlation appeared with condensed tannins, referring only to R^2 . Similar results were found by [44] with a good trend between the total phenol profile and the antioxidant activity of the plant extracts, suggesting that phenolic compounds are responsible for the antioxidant activity of those extracts.

However, our perception of the analysis of these results must in no way be based on the simple data of R^2 but also on the basis of p -values. Indeed, the different values obtained were 20.47%, 16.80%, and 4.12% for TPC, TFC, and CT, respectively (cf. Figure 3). Following these results, it thus appears clearly that the p -values exceeded by far the 5% tolerated, so that a model was retained as a linear regression model except for the case of CT. Thus, the quality of the model reflecting the linear dependence between IC_{50} and CT was the best and those corresponding to TPC and TFC were rejected, notwithstanding the higher values of R^2 .

3.8. Anticorrosion activity

3.8.1. PP measurements

PP measurements were made at 308 K after 30 min of immersion at open circuit potential in the presence or absence of 0.01 g L^{-1} of various *A. visnaga* extracts in order to acquire information on the kinetics of anodic and cathodic reactions. Fig. 4 illustrates the current–potential characteristics of mild steel in 1 M HCl solution. The choice of this concentration was dictated by the maximum of inhibition efficiency when compared with the other explored concentrations (not reported here).

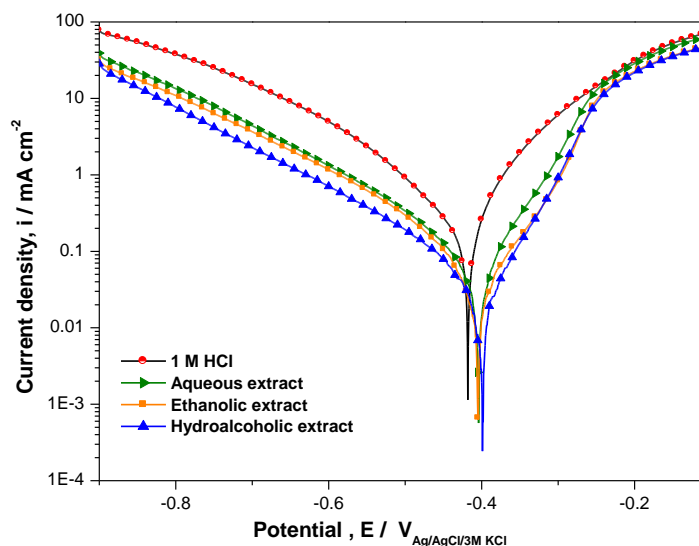


Figure 4. Steady-state polarization curves for mild steel in 1 M HCl in the absence or presence of 0.01 g L^{-1} of different extracts of *A. visnaga*.

Figure 4 shows that the addition of different extracts of *Ammi visnaga* in the acid solution reduced the anode and cathode branches compared with the control solution. This indicates that both the hydrogen reduction reactions and the dissolution of the metal were slowed down. Besides, the cathodic active sites of mild steel can be covered by phenolic molecules at 0.01 g L^{-1} with *Ammi visnaga* extracts.

According to Figure 4, the cathodic curves showed Tafel behavior, which shows that the mechanism for reducing H^+ ions at the cathode surface sites of mild steel is through a charge transfer mechanism.

The cathodic branch of the polarization curves for the three extracts of *Ammi visnaga* was shifted, indicating that the chemical constituents of the extracts had a separate effect on the cathodic process. In addition, the different extracts affected the anodic branch at different degrees, indicating that their inhibitive effect depended on the type of solvent only at over potential lower than -0.3 V vs. Ag/AgCl, 3 M KCl. The anodic shift for steel in the presence of different extracts was in the following order: hydroalcoholic > ethanolic > aqueous.

The electrochemical parameters, such as corrosion current density i_{corr} , corrosion potential E_{corr} , cathodic Tafel slope β_c , and inhibition efficiency $\eta_{pp}\%$ are given in Table 5. Inhibition efficiency $\eta_{pp}\%$ was calculated from the corrosion current density values according to Equation (3):

$$\eta_{pp}\% = \frac{i_{corr} - i_{corr}^{inh}}{i_{corr}} \times 100 \quad (3)$$

where i_{corr} and i_{corr}^{inh} are the corrosion current densities of mild steel in the absence or presence of different extracts of *A. visnaga*, respectively.

Table 5. Electrochemical parameters of mild steel in 1 M HCl solution without and with different extracts of *A. visnaga*.

$C_{inh} = 0.01 \text{ g L}^{-1}$	E_{corr} mV _{Ag/AgCl, 3 M KCl}	i_{corr} $\mu\text{A cm}^{-2}$	$ \beta_c $ mV dec ⁻¹	$\eta_{pp}\%$
1 M HCl	-416.236	337.06	159.4	-
Aqueous	-404.293	91.20	166.4	72.94
Ethanolic	-404.907	79.12	163.9	76.52
Hydroalcoholic	-399.466	49.81	172.1	85.22

The analysis of Table 5 shows that corrosion current densities decreased considerably with the addition of different extracts of *A. visnaga*. As a result, the hydroalcoholic extract gave the highest inhibitory efficacy of 85.22% when compared with ethanolic extract (76.52%) and aqueous (72.94%). These results suggest that the protective adsorption film formed onto the surface of mild steel tended to be increasingly high and stable with the addition of the hydroalcoholic extract. The addition of different inhibitors caused a slight shift in corrosion potential compared with that without an inhibitor. In this study, the corrosion potential moved anodically between 12 and 17 mV compared with the solution without an inhibitor. Based on literature reports, if the displacement of corrosion potential is greater than 85 mV, the inhibitor can be considered as a cathodic or anodic type inhibitor, while when the displacement is less than 85 mV, the inhibitor can be classified as a mixed type inhibitor [49]. Accordingly, the obtained results revealed that the extracts here acted as mixed-type inhibitors.

3.8.2. EIS measurements

The EIS measurements were performed to obtain information on the elementary steps that make up the overall electrochemical process. Fig. 5 shows the Nyquist diagram after 30 nm of immersion of the mild steel in an acid medium at an open circuit in the presence or absence of the various extracts of *A. visnaga*. The impedance diagrams were performed over the frequency range of 100 kHz to 100 mHz. The recorded EIS spectra for mild steel in 1 M HCl at 308 K showed one depressed capacitive loop.

A similar trend (a capacitive loop) was also noticed for mild steel immersed in 1 M HCl containing 0.01 g L^{-1} of different extracts. Further, the above impedance diagrams were in the form of a depressed semicircle, the center of which was located under the real axis, showing that the overall corrosion process was controlled by the charge transfer step. Such behavior is characteristic of solid electrodes and is generally ascribed to Cole–Cole [50, 51] and/or Cole–Davidson [52] representations inherent to frequency dispersion. This phenomenon is generally attributed to different physical processes such as the nonhomogeneity of the electrode surface or its roughness during the corrosion process, adsorption of inhibitors, and formation of porous layers [49].

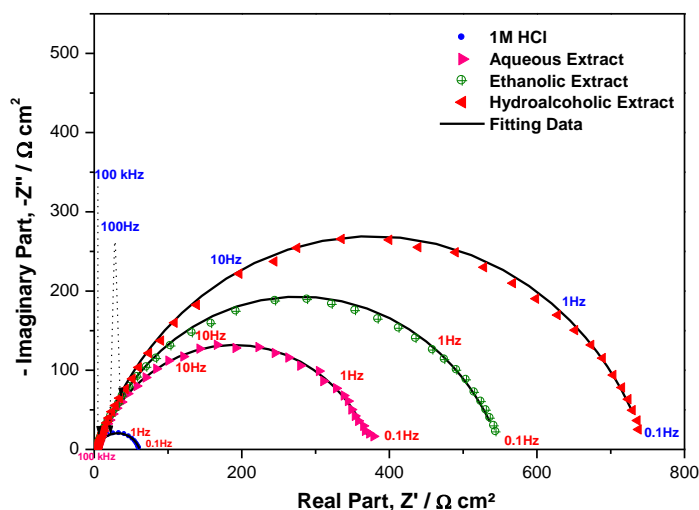


Figure 5. Nyquist diagrams of mild steel in 1 M HCl in the absence or presence of different extracts of *A. visnaga*.

Fig. 5 shows that the diameter of R_{ct} increased after the addition of different extracts to the corrosive solution [50]. This increase became more and more pronounced with addition of hydroalcoholic extract, which indicates more adsorption of phenolic compounds on the metal surface when compared with ethanolic and aqueous extracts, respectively.

In order to confirm the proposed mechanism, it would be very practical to draw Bode diagrams that explicitly show frequency information at high frequencies. The mild steel Bode diagrams, which were obtained in a 1 M HCl solution with or without different extracts of *A. visnaga*, are given in Fig. 6.

The Bode diagram presented in the Fig. 6 is characterized by the presence of a single oblique slope, a single time constant, and a single maximum in the intermediate frequencies on the diagrams (\log

$f - \log |Z|$) and $(\log f - \varphi)$, respectively, which proves that corrosion in 1 M HCl mild steel solution was mainly controlled by a charge transfer process ($R_P = R_{ct}$) [49].

A detailed analysis of the $(\log f - \log |Z|)$ and $(\log f - \varphi)$ on mild steel indicated the existence of three main regions. In the first one (1), at high frequencies ranging from 4 to 100 kHz, the impedance modulus $|Z|$ as well as the phase angle φ were very low, corresponding to an ohmic resistance R_s of the electrolytic solution (1 M HCl) between the working and reference electrodes. The second region (2), between 3 Hz to 4 kHz, showed a linear dependence of $\log |Z| - \log f$ with a slope, $\partial(\log |Z|) / (\partial \log f)$, and a phase angle φ far from -1° and 90° , respectively, reflecting then a nonideal condenser [53-55] corresponding to the capacitance of the mild steel/solution interface (in the absence or presence of different extracts of *A. visnaga* in the solution). For region (3), corresponding to low frequencies (from 0.1 to 3 Hz), the impedance modulus $|Z|$ was again practically independent of frequency and was accompanied by an abrupt decrease of the phase angle $\varphi \rightarrow 0$. Thus, the impedance modulus $|Z|$ in this region corresponded to the sum of the charge transfer and the electrolytic resistance ($|Z| = R_{ct} + R_s$). Evidently, regions 1 and 3 showed typical ohmic behavior, with $|Z_1| = R_s$ and $|Z_3| = R_{ct} + R_s$, respectively.

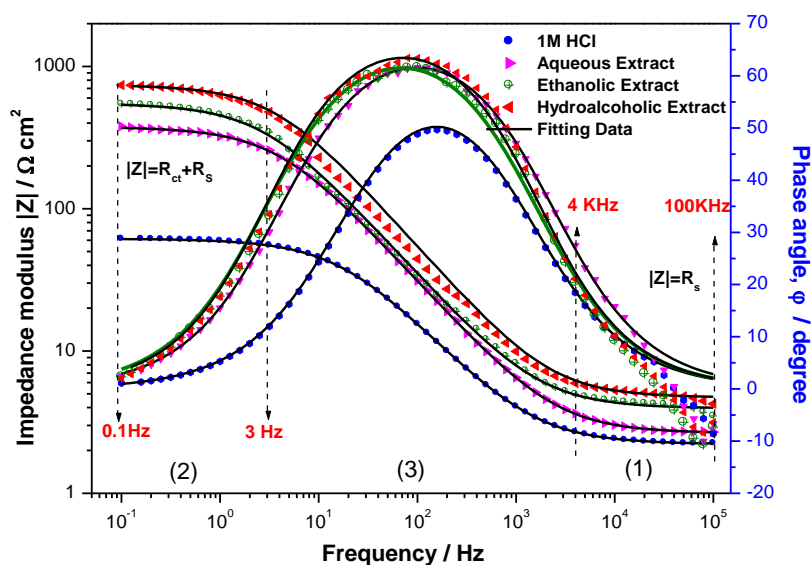


Figure 6. Bode diagrams for mild steel in 1 M HCl solution at different extracts of *A. visnaga* at 308 K.

Based on the analysis of the Nyquist and Bode diagrams, the simulations of impedance diagrams with the modified Randles model containing a constant phase element *CPE*, instead of a double layer capacitance in parallel to the load transfer resistance R_{ct} , were all in a series with another resistance corresponding to the resistance of the electrolyte solution R_s , which showed excellent agreement with the experimental data. This equivalent circuit proposed for the studied interface is shown in Fig. 7.

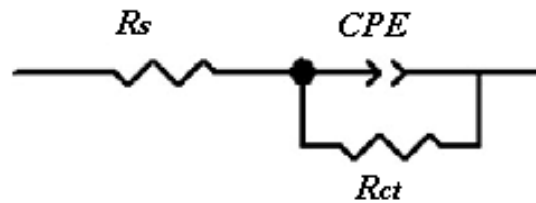


Figure 7. Equivalent circuit model.

The impedance of CPE is defined by the mathematical expression [45,51] given in Equation (4):

$$Z_{CPE} = \frac{1}{Q(j\omega)^n} = \frac{1}{Q \times \omega^n} e^{\left(\frac{-j \times \pi \times n}{2}\right)} = \frac{1}{Q \times \omega^n} \left(\cos\left(\frac{\pi \times n}{2}\right) - j \times \sin\left(\frac{\pi \times n}{2}\right) \right) \tag{4}$$

where Q is a proportional factor (in $\mu F s^{n-1} cm^{-2}$), j is an imaginary number with $j^2 = -1$, n is an exponent related to the phase shift, ω is the angular frequency in rad^{-1} ($\omega_{max} = 2 \times \pi \times f_{max}$), and f_{max} is the frequency of which the imaginary component of the impedance is maximal.

The double layer pseudo capacitance C_{dl} was calculated by Equation (5) according to [49,54]:

$$C_{dl} = (Q \times R_{ct}^{1-n})^{1/n} \tag{5}$$

The R_{ct} was used to calculate the inhibition efficiency $\eta_{EIS}\%$ of different extracts of *Ammi visnaga*, given by Equation (6):

$$\eta_{SIE} \% = \frac{R_{tc}^{inh} - R_{tc}}{R_{tc}^{inh}} \times 100 \tag{6}$$

where R_{ct} and R_{ct}^{inh} are the charge transfer resistances without or with different extracts of *A. visnaga*, respectively.

Table 6. Impedance parameters of mild steel in 1 M HCl in the absence or presence of 0.01 g L⁻¹ of different extracts of *A. visnaga*.

C_{inh} g L ⁻¹	R_s Ωcm^2	R_{ct} Ωcm^2	C_{dl} $\mu F cm^{-2}$	Q $\mu F s^{n-1} cm^{-2}$	n	χ^2	η_{EIS} %
Blank	2.19 ±0.23	59.47±0.37	149.9	180.2±2.2	0.7672	0.011	-
Aqueous	2.63±0.21	374.80±0.31	103.8	211.3±9.1	0.7812	0.001	84.14
Ethanollic	3.93±0.27	547.30±0.47	100.8	189.6±5.3	0.7819	0.003	89.13
Hydroalcoholic	4.7 ±0.11	738.71±0.56	72.7	130.1±1.7	0.7986	0.006	91.94

* Data are expressed as means ± standard deviation of fitting data

The various calculated parameters, such as R_{ct} , C_{dl} , n , R_s , Q , χ^2 , and $\eta_{EIS}\%$, are shown in Table 6. The χ^2 , given in Equation 7, used in this method is defined as follows [49]:

$$\chi^2 = \sum_{i=1}^n \frac{|Z_{meas}(i) - Z_{model}(f_i, param)|^2}{D_i^2} \tag{7}$$

where $Z_{meas}(i)$ is the measured impedance at the f_i frequency, $Z_{model}(f_i, param)$ is a function of the chosen model, $param$ is the model parameter (R_s, R_{ct}, Q), and D_i is the standard deviation. Estimates of the margins of error calculated for some parameters are also reported in Table 6.

Table 1 shows that the quality of fitting to the equivalent circuit was judged by the chi-squared value χ^2 [56]. The corresponding values (0.011–0.001), reported in Table 6, demonstrate the good quality fitting with the proposed circuit.

Inspection of the impedance data corresponding to the three extracts reported in Table 6 revealed that the R_{ct} of the mild steel increased considerably after the addition of 0.01 g L⁻¹ of different extracts (aqueous, ethanolic, or hydroalcoholic) to 1 M HCl solution and attained a maximum value of 738 Ω cm² in the presence of the hydroalcoholic extract, followed by the ethanolic (547 Ω cm²) and aqueous (374 Ω cm²) extracts. The value of the Q parameter of CPE and also the pseudocapacity of the double layer C_{dl} decreased, which could have been due to an increase in the thickness of the double layer and/or a decrease in local dielectric constant. This may be due to the progressive replacement of ions and water molecules adsorbed on the surface by the adsorption of inhibiting molecules on the metal surface [49,55,56].

Furthermore, the excellent inhibitory properties of the hydroalcoholic extract can be interpreted as being the result of the intense presence of adsorbent phenolic molecules in the hydroalcoholic extract when compared with the ethanolic and aqueous extracts.

The present study shows for all EIS spectra that $n < 1$, with or without different extracts, showing the surface heterogeneity despite the adsorption of the inhibitor molecules contained in the different extracts on the active adsorption sites of the electrode surface.

3.8.3. Correlation between phenolic compounds and inhibition efficiency

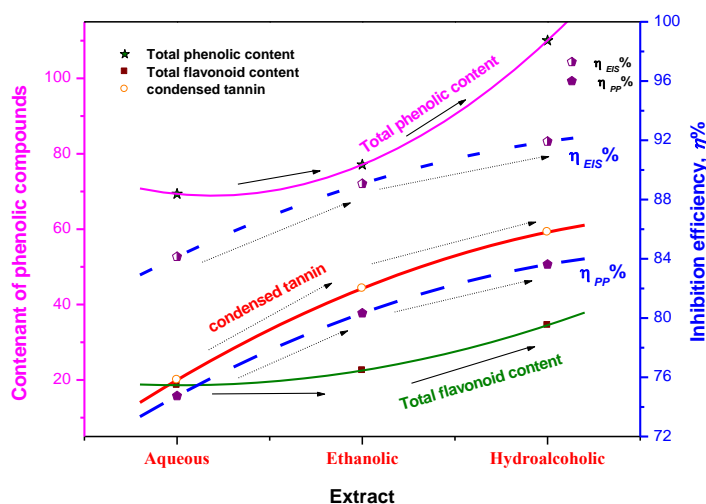


Figure 8. Data trends of phenolic compounds and inhibition efficiency $\eta\%$.

The relationships between phenolic compounds and inhibitive actions were analyzed by comparing the trends of phenolic compounds to those of inhibition efficiency by Origin. The graphs of TPC, TFC, CT, and $\eta\%$ (obtained from the Tafel and EIS techniques) are given in Fig. 8.

The TPC, TFC, and CT are expressed as a percentage to allow direct comparison of phenolic profiles with $\eta_{PP}\%$ and $\eta_{EIS}\%$ curves. It is obvious from Figure 8 that the evolution of CT in the three extracts followed the same trend as the inhibition efficiency $\eta\%$ obtained from both Tafel and EIS measurements, whereas others tendencies were registered with TPC and TFC. Thus, it can easily be concluded that the inhibitory properties of *A. visnaga* may be attributed to condensed tannin present in extracts.

3.8.4. Relation between antioxidant and inhibition efficiency of *A. visnaga* extracts

The relationships between IC_{50} and inhibition efficiency $\eta\%$ (calculated from i_{corr} and R_{ct}) were analyzed by comparing the trends of IC_{50} and those of inhibition efficiency by Origin 6.0. The correlation between IC_{50} and inhibition efficiency in the three extracts are plotted in Fig. 9.

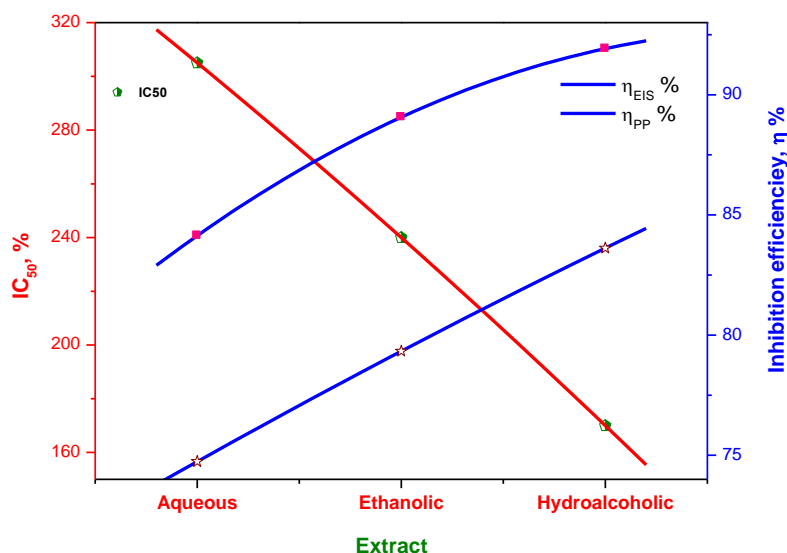


Figure 9. Data trends of antioxidant activity and inhibition efficiency ($\eta\%$).

Fig. 9 shows that the IC_{50} values decreased considerably with the hydroalcoholic extract when compared with the ethanolic and aqueous extracts, respectively. As opposed to this trend, the corrosion inhibition efficiency increased. In addition, the strong correlation between CT and IC_{50} as well as CT and inhibition efficiency reported in Figs. 3 and 8, respectively, as well as the strong presence of CT in the hydroalcoholic extract with the highest content (65.20 mg of catechin/g extract) when compared with the other extracts (cf. Table 2), can be attributed to their increased solubility, which is likely inherent to the decreased polarity of the hydroalcoholic solvent.

Consequently, all these results illustrate a similar trend between antioxidant and anticorrosive activities and their strong dependence on the CT content.

4. CONCLUSION

This study showed that the extraction solvent had a significant effect on the phenolic profiles of different extracts of *A. visnaga* and therefore on antioxidant activity.

The results showed that hydroalcoholic extraction gave the maximum yield. Quantitative analysis showed that the hydroalcoholic extract had the the highest TPC, TFC, and CT when compared with the ethanolic and aqueous extracts, thus providing an intense capacity to trap free radicals.

The correlation between the phenolic compounds (TPC, TFC, and CT) and IC_{50} of the different extracts showed that the condensed tannin content of the different extracts was very well correlated with IC_{50} .

The electrochemical analysis suggested that different extracts of *A. visnaga* have an inhibition action in acidic media. A good trend was obtained between the corrosion inhibition properties of *A. visnaga* extracts and their total phenolic content and antioxidant activity.

References

1. A. E. Al-Snafi, *Int. J. Pharm. & Ind.*, 3 (2013) 257.
2. M. H. A. El Gamal, N. M. M. Shalaby, H. Duddeck and M. Hiegemann, *Phytochemistry*, 34 (1993) 819.
3. J.B.Harborne and L. King, *Biochem. Syst. Ecol.*, 4 (1976) 111.
4. A.N. Singab, *Phytochemistry*, 49 (1998) 2177.
5. T. Z. Abdul Jalil, K. Saour and A. M. A. Nasser, *J. Pharm. Sci.*, 19 (2010) 48.
6. K. Günaydın and F. B. Erim, *J. Chromatogr. A*, 954 (2002) 291.
7. K. W. Tan and M. J. Kassim, *Corros. Sci.*, 53 (2011) 569.
8. Y. Cai, Q. Luo, M. Sun and H. Corke, *Life Sci.*, 74 (2004) 2157.
9. H. R. Jadhav and K. K. Bhutani, *Phytother. Res.*, 16 (2002) 771.
10. I. F. F. Benzie and J. J. Strain, *Anal. Biochem.*, 239 (1996) 70.
11. B. Auddy, M. Ferreira. F. Blasina, L. Lafon, F. Arrendondo, F. Dajas, P. Tripathy, T. Seal and B. Murkerjee, *J. Ethnopharmacol.*, 84 (2003) 131.
12. I. N. Putilova, S. A. Balezin and V. P. Barannik, *Pergamon. Press. New York* (1960) p. 31.
13. M. A. Amin, S. S. Abd El-Rehim, E. E. F. El-Sherbini and R. S. Bayoumi, *Electrochim. Acta*, 52 (2007) 3588.
14. B. Labriti, N. Dkhireche, R. Touir, M. EbnTouhami, M. Sfaira, A. El Hallaoui, B. Hammouti and A. Alami, *Arab. J. Sci. Eng.*, 37 (2012) 1293.
15. B. Zerga, B. Hammouti, M. EbnTouhami, R. Touir, M. Taleb, M. Sfaira, M. Bennajeh and I. Forssal, *Int. J. Electrochem. Sci.*, 7 (2012) 471.
16. K. Benbouya, B. Zerga, M. Sfaira, M. Taleb, M. Ebn Touhami, B. Hammouti, H. Benzeid and E. M. Essassi, *Int. J. Electrochem. Sci.*, 7 (2012) 6313.
17. B. Zerga, M. Sfaira, Z. Rais, M. Ebn Touhami, M. Taleb, B. Hammouti, B. Imelouane and A. Elbachiri, *Mater. Tech.*, 97 (2009) 297.
18. L. Afia, R. Salghi, L. Bammou, El. Bazzi, B. Hammouti, L. Bazzi and A. Bouyanzer, *J. Saudi Chem. Soc.*, 18 (2014) 19.
19. J. Bhawsar, P. K. Jain and P. Jain, *Alex. Eng. J.*, 54 (2015) 769.
20. M. R. Singh, P. Gupta and K. Gupta, *Arab. J. Chem.*, 52 (2015) 1878.
21. A. K. Satapathy, G. Gunasekaran, S. C. Sahoo, K.Amit and P. V. Rodrigues, *Corros. Sci.*, 51 (2009) 2848.

22. P. C. Okafor, M. E. Ikpi, I. E. Uwah, E.E. Ebenso, U. J. Ekpe and S. A. Umoren, *Corros. Sci.*, 50 (2008) 2310.
23. A. Y. El-Etre, *Appl. Surf. Sci.*, 252 (2006) 8521.
24. M. D. Judith, Thèse de doctorat en pharmacie de l'Université de BAMAKO (2005) 57.
25. N. Dohou, K. Yamni, S. Tahrouch, L. M. Idrissi Hassani, A. Badoc and N. Gmira, *Soc. Pharm. Bordeaux*, 142 (2003) 61.
26. A. Diallo, Thèse de pharmacie. Faculté de Médecine, de Pharmacie et d'Odonto-Stomatologie (Fmpos). Université de Bamako (2005).
27. E. K. Akkol, F. Göger, M. Kosar and K. H. Başer, *Food Chem.*, 108 (2008) 942.
28. C. Quettier-Deleu, B. Gressier, J. Vasseur, T. Dine, C. Brunet, M. Luyckx, M. Cazin, J. C. Cazin, F. Bailleul and F. Trotin, *J. Ethnopharm.*, 72 (2000) 35.
29. B. Sun, J. M. Richardo-Da-Silvia and I. Spranger, *J. Agric. Food Chem.*, 46 (1998) 4267.
30. K. Shimada, K. Fujikawa, K. Yahara and T. Nakamura, *J. Agric. Food Chem.*, 40 (1992) 945.
31. P. Prieto, M. Pineda and M. Aguilar, *Anal. Biochem.*, 269 (1999) 337.
32. S. Bourgou, B. R. Serairi, F. Medini and R. Ksouri, *Agr. Bio. Tech.*, 28 (2016).
33. Z. Mohammedi and F. Atik, *Int. J. Pharma. Bio. Sci.*, 2 (2011) 609.
34. K. Ammor, D. Bousta, S. Jennan, A. Chaqroune and F. Mahjoubi, *Der Pharma Chemica*, 9 (2017) 73.
35. S. Aourabi, M. Driouch, K. Ammor, M. Sfaira, M. Ebn Touhami and F. Mahjoubi, *Anal. Bioanal. Electrochem.*, 10 (2018) 912.
36. M. Alothman, R. Bhat and A. A. Karim, *Food Chem.*, 115 (2009) 785.
37. S. F. Sulaiman, A. A. B. Sajak, K. L. Ooi, Supriatno and E. M. Seow, *J. Food Compos. Anal.*, 24 (2011) 506.
38. A. Wojdylo, J. Oszmianski and R. Czemerys, *Food Chem.*, 105 (2007) 940.
39. S. Jennan, A. Farah and F. Mahjoubi, *J. Mater. Environ. Sci.*, 6 (2015) 773.
40. R. Petlevski, D. Flajs, Z. Kalodela and M.Z. Končić, *S. AFR. J. BOT.*, 85 (2013) 17.
41. B. Lapornik, M. Prosek and A. G. Wondra, *J. Food Eng.*, 71 (2005) 214.
42. K. Shimada, K. Fujikawa, K. Yahara and T. Nakamura, *J. Agric. Food Chem.*, 40 (1992) 945.
43. L. R. Fukumoto and G. Mazza, *J. Agric. Food Chem.*, 48 (2000) 3597.
44. J. R. Soares, T. C. P. Dins, A. P. Cunha and L. M. Almeida, *J. Free Radic. Res.*, 26 (1997) 469.
45. A. Pizzi, *Ind. Eng. Chem. Prod. Res. Devel.*, 21 (1982) 359.
46. S. Moreno, T. Scheyer, C.S. Romano and A.A. Vojnov, *J. Free Rad. Res.*, 40 (2006) 223.
47. Y. Gong, X. Liu, W. H. He, H. G. Xu, F. Yuan and Y. X. Gao, *Fitoterapia*, 83 (2012) 481.
48. D. Karou, M. H. Dicko, J. Simporé and A. S. Traore, *Afr. J. Biotechnol.*, 4 (2005) 823.
49. M. Beniken, M. Driouch, M. Sfaira, B. Hammouti, M. Ebn Touhami and M. A. Mohsin, *J. Bio. Tribo-Corros.*, 4 (2018) 38.
50. K. S. Cole and R. H. Cole, *J. Chem. Phys.*, 9 (1941) 341.
51. S. Duval, M. Keddou, M. Sfaira, A. Srhiri and H. Takenouti, *J. Electrochem. Soc.*, 149 (2002) 520.
52. D. W. Davidson and R. H. Cole, *J. Chem. Phys.*, 19 (1951) 1484.
53. D. A. Lopez, S. N. Simison and S. R. Sanchez, *Corros. Sci.*, 47 (2005) 735.
54. M. Lebrini, F. Robert, H. Vezin and C. Roos, *Corros. Sci.*, 52 (2010) 3367.
55. M. Beniken, M. Driouch, M. Sfaira, B. Hammouti, M. Ebn Touhami and M. A. Mohsin, *J. Bio. Tribo-Corros.*, 4 (2018) 34.
56. Z. Bensouda, M. Driouch, M. Sfaira, A. Farah, M. Ebn Touhami, B. Hammouti, K.M. Emran, *Int. J. Electrochem. Sci.*, 13 (2018) 8198.